

# Photophysical studies of neutral aromatic species confined in zeolite L: Comparison with cationic dyes†

Shuichi Hashimoto,<sup>\*a</sup> Masahide Hagiri,<sup>a</sup> Nobukazu Matsubara<sup>a</sup> and Seiji Tobita<sup>b</sup>

<sup>a</sup> Chemistry Department and Advanced Engineering Courses, Gunma College of Technology, Maebashi, Gunma 371-8530, Japan

<sup>b</sup> Department of Chemistry, Gunma University, Kiryu, Gunma 376-8515, Japan

Received 11th June 2001, Accepted 17th September 2001

First published as an Advance Article on the web

The photophysical properties of a few aromatic molecules incorporated into the straight channels of zeolite L were investigated, mainly by luminescence spectroscopy. Two significant observations were made. (1) Intense room temperature phosphorescence (RTP) was observed for 9-ethylcarbazole and other aromatics included in the dehydrated K<sup>+</sup>-form of the zeolite L (KL) whereas RTP was very weak in 47 atom % Na<sup>+</sup>-exchanged KL (NaKL) and the K<sup>+</sup>- and Na<sup>+</sup>-forms of zeolite Y (KY and NaY). Previously, observation of RTP was only made in zeolites exchanged with heavy atom cations such as Rb<sup>+</sup> and Cs<sup>+</sup>. For 9-ethylcarbazole, the tight fit into the KL channels and resultant increased structural rigidity are largely responsible for the remarkable reduction in the rate of nonradiative intersystem crossing from T<sub>1</sub> to S<sub>0</sub>, leading to the enhanced phosphorescence lifetime even at room temperature. (2) Anthracene, intercalated in the channels, formed dimers that can be detected by the excimer emission. It was found that the dimer formed in NaKL has less overlap than that formed in KL. Moreover, the dimer must have a remarkably short separation between the two rings, comparable to that of anthracenophane, judging from its distorted absorption spectrum. Formation of naphthalene dimers with partial overlap in KL was identified from the characteristic fluorescence spectrum of the second excimer. No naphthalene dimer was formed in NaKL even at high loadings. Thus the photophysics of anthracene and naphthalene in zeolite L is remarkably different from that in solutions and large-pore faujasite zeolites where the framework exerts only weak conformational control over the guest molecules. Additionally, the charge compensating cations in zeolite L were found to have the ability to control the distribution and conformation of the guest species within the channels. The present findings show that the zeolite L is a better host matrix than the large pore faujasite zeolites for manipulating the photophysics of neutral guest species.

## Introduction

Photochemistry in zeolites has attracted increasing attention in recent years since they can host many organic molecules in their cavities and channels and thereby modify their properties.<sup>1</sup> In most cases, the large pore (1.3 nm in diameter) faujasite zeolites, X and Y, that can incorporate organic molecules with dimensions as large as 0.74 nm, were utilized. Channel-type zeolite L has also been employed recently in photochemical research.<sup>1e,1g</sup> The channels are characterized by a 0.71 nm diameter opening consisting of 12-membered ring oxygens and the unit cell is 1.3 nm × 0.75 nm (Chart 1). Thus the channels are of a size to fit molecules with a short axis length smaller than that of substituted benzenes and thus may exclude molecules with much larger dimensions. The advantage of the channels of zeolite L over the spherical supercages is the greater structural control enforced on the guest species by the channel walls since the guest species are forced to align in a collinear geometry along the narrow cylinders.<sup>1e</sup> Additionally, it has been suggested that the guest species are distributed fairly uniformly throughout the channels.<sup>1e</sup> In contrast, the distribution of guest molecules in faujasite supercages is appreciably heterogeneous and the large spher-

ical hollow shape allows considerable room for movement of the molecules impregnated from solution or by sublimation.

Cationic dyes, Methylviologen (MV<sup>2+</sup>)<sup>2</sup> and Thionine (TH<sup>+</sup>),<sup>3</sup> that are smaller than the channel diameter were incorporated into KL *via* cation exchange. It was suggested that the TH<sup>+</sup> molecules are adsorbed in a monomeric form even at high loadings, whereas the slightly larger Methylene Blue (MB<sup>+</sup>) molecules were adsorbed on the exterior surfaces, forming dimers and aggregates.<sup>3</sup> These organic dyes have the tendency to form aggregates at relatively low concentrations in aqueous solution but the geometry of the channels of zeolite L does not allow the formation of parallel dimers (H-type aggregates). Other studies have shown<sup>4</sup> that on photoexcita-

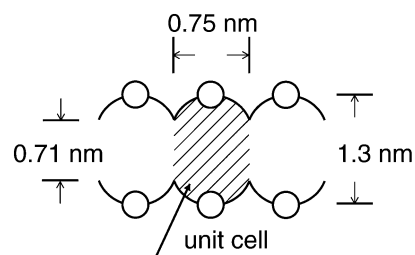


**Chart 1** Cross sectional view of zeolite L main channel. The dimensions of the channels are depicted in the Chart. Cations buried in the channel walls are indicated by small circles.

† Electronic Supplementary Information available. See <http://www.rsc.org/suppdata/cp/b1/b105100h/>

tion of  $MV^{2+}$  in various zeolites the radical cations of  $MV^{2+}$  ( $MV^{\cdot+}$ ) are formed through a photoinduced electron transfer from the electron-donating sites of the zeolites to the excited singlet-state of  $MV^{2+}$ . Interestingly, the dimerization of  $MV^{\cdot+}$  to form  $(MV^{\cdot+})_2$  was observed exclusively in zeolite L (not in zeolite Y) when incorporated into dehydrated zeolites.<sup>5</sup> Furthermore, Förster-type energy transfer between two cationic dyes, from Pyronine ( $Pyr^+$ ) to Oxonine ( $Oxo^+$ ) in the channels was observed by Calzaferri's group to proceed very efficiently.<sup>6</sup> In the meantime, the aggregation of the dyes in solution caused fast thermal relaxation of electronic excitation energy. Thus, they proposed that the dye-loaded zeolite L is a promising candidate for a light-harvesting antenna system mimicking plants. Overall, zeolite L is well suited for photophysical and photochemical applications utilizing cationic dyes.

By contrast, only a few studies have explored the photochemistry of neutral aromatic species in zeolite L. A photophysical study of pyrene by Thomas' group<sup>7a</sup> has shown that pyrene molecules adsorb on the external surfaces of zeolite L owing to their larger molecular size, forming dimers in the ground state. On the other hand, "slim" molecules such as biphenyl and *p*-terphenyl were incorporated inside the channels<sup>7b</sup> and were studied by Raman spectroscopy. It turned out that the method is not very sensitive to the detection of the interplay of the zeolite framework with the guest species and the mutual interaction of the adsorbed species. The lack of information about neutral species inside zeolite L prompted us to investigate the confinement effect by the channel walls on aromatic molecules such as biphenyl, naphthalene and anthracene, which are just small enough to fit into the main channel. Emission spectroscopic techniques<sup>8,9</sup> were applied to investigate the adsorption interaction and photophysical properties of these neutral guest species intercalated in the channel-type zeolite L. The role of the zeolite is discussed as a container that can fix molecules so remarkably, as in low temperature solid media, so as to allow phosphorescence emission at room temperature and also can enforce molecules to associate to form dimers of various geometry, depending on the cations, even in the narrow channels.

## Experimental

9-Ethylcarbazole, ECZ (Tokyo Kasei, >99%) was recrystallized three times from ethanol. Naphthalene (Tokyo Kasei, zone refined), phenanthrene (Tokyo Kasei, zone refined) and anthracene (Merck, scintillation grade) were used as received. Biphenyl (Wako Chemicals) was recrystallized. n-Hexane (Wako chemicals, HPLC grade) was distilled and stored over 4A molecular sieves. Zeolite KL (unit cell  $Na_{0.2}K_{8.8}Al_{9.0}Si_{27}O_{72} \cdot xH_2O$ ) and NaY (unit cell  $Na_{50.5}Al_{50.5}Si_{141.5}O_{384} \cdot xH_2O$ ) were kindly provided by Tosoh. Cation-exchanged zeolites were prepared *via* ion-exchange of KL and NaY according to the procedure described in the literature.<sup>2b,5</sup> The zeolite powder was calcined in air at 500 °C for *ca.* 8 h just before sample preparation.

Incorporation of aromatic molecules into the dried zeolites was carried out by adding n-hexane solutions of each molecule to the zeolite powders. The aromatics-zeolite mixture was stirred at room temperature for a few minutes; the sample was filtered. Then, the powders were washed twice with n-hexane and vacuum dried. The unadsorbed aromatic molecules in the supernatant solutions were assayed spectrophotometrically. All the procedures were carried out in a nitrogen-filled glovebox. The samples were transferred into 2 mm thick Suprasil cells and were evacuated at <0.4 Pa for 12 h at 100 °C. Additionally, sublimation of the aromatics in vacuum (<0.4 Pa) was carried out for adsorption into the dehydrated zeolites.<sup>9a</sup>

The ground-state reflectance spectra were measured on a Shimadzu UV-3101PC double-monochromator spectro-

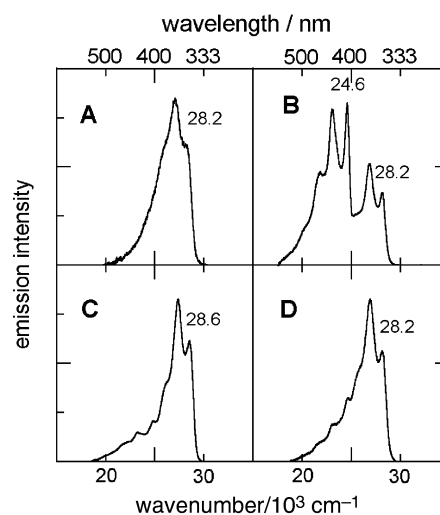
photometer equipped with an integrating sphere coated with  $BaSO_4$ . The reference was  $BaSO_4$  (Kodak white reflectance standard). Absorption spectra of ground state species were obtained by using the Kubelka-Munk function. Fluorescence spectra were obtained with a Hitachi F-3010 spectrofluorometer. The spectral response of the fluorometer was corrected with fluorescence standards.<sup>10</sup> Fluorescence decay curves were recorded on a time-correlated single-photon-counting apparatus (Edinburgh Analytical Instruments, FL900CDT). Here a nanosecond pulsed discharge lamp (pulse width 1 ns, repetition rate 40 kHz) filled with hydrogen gas was used as an excitation light source. Transient absorption spectra and phosphorescence decays were measured on a diffuse reflectance laser photolysis set-up described previously.<sup>1h</sup>

## Results and discussion

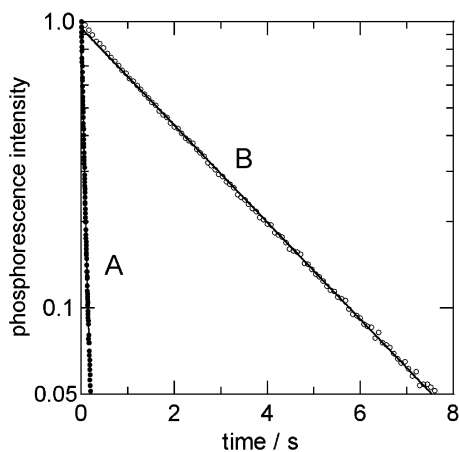
### 1. Room-temperature phosphorescence (RTP) of 9-ethylcarbazole included in zeolite KL

Fig. 1 compares the emission spectrum of 9-ethylcarbazole (ECZ) adsorbed in zeolite KL with that in zeolite KY (98 atom %  $K^+$ ) at a low loading level of  $2.0 \times 10^{-6} \text{ mol g}^{-1}$  at 296 K. The emission spectra in NaY and NaKL (47 atom %  $Na^+$ -exchanged zeolite KL) are also given in Fig. 1. Remarkably, the phosphorescence of ECZ was observed in KL while it was only very weakly detected in zeolite KY. However, the present observation in zeolite KL is different from the previously reported heavy atom assisted phosphorescence<sup>11</sup> and unique to zeolite L because the least heavy atom effect is anticipated for  $K^+$  ions from the value of their spin-orbit coupling constant.<sup>11a</sup> Neither can any heavy atom effect be expected for impurities contained in the zeolite: much less than the 100 ppm of Fe, Ni, Cr ions that normally act as luminescence quenchers were detected in the zeolites NaY and KY as well as in zeolite KL. Accordingly, the structure of the zeolite is decisive for the present observation based on the fact that the phosphorescence of ECZ is very weak in the zeolite KY possessing the same charge compensating cations as zeolite KL.

The mechanistic aspect of the increased phosphorescence emission in zeolite KL was investigated. Enhanced phosphorescence can be observed on the basis of three factors, an increased quantum yield of intersystem crossing from  $S_1$  to  $T_1$



**Fig. 1** Corrected emission spectra of  $2.0 \times 10^{-6} \text{ mol g}^{-1}$  9-ethylcarbazole adsorbed in various zeolites at 296 K (excitation wavelength: 290 nm ( $34\,500 \text{ cm}^{-1}$ )): (A) zeolite KY; (B) zeolite KL; (C) zeolite NaY; (D) zeolite NaKL. No cut-off filters were used for the measurements.



**Fig. 2** Phosphorescence decay curves of  $2.0 \times 10^{-6}$  mol  $\text{g}^{-1}$  9-ethylcarbazole adsorbed in KY (A) and KL (B) at 296 K, excited at 337 nm ( $29\,700\text{ cm}^{-1}$ ) and observed at 435 nm ( $23\,000\text{ cm}^{-1}$ ). The decay constants are  $15\text{ s}^{-1}$  for A and  $0.39\text{ s}^{-1}$  for B. The RC time constant of the detection system is less than 150  $\mu\text{s}$ .

( $\Phi_{\text{ST}}$ ), an enhanced radiative rate of phosphorescence ( $k_{\text{P}}$ ) and an increased phosphorescence lifetime since the quantum yield of phosphorescence,  $\Phi_{\text{P}}$  is represented by:<sup>12</sup>

$$\Phi_{\text{P}} = \Phi_{\text{ST}} \frac{k_{\text{P}}}{(k_{\text{P}} + k_{\text{D}})} = \Phi_{\text{ST}} k_{\text{P}} \tau_{\text{T}}$$

where  $k_{\text{D}}$  represents the rate constant for unimolecular radiationless deactivation of  $\text{T}_1$ , and  $\tau_{\text{T}}$ : a phosphorescence lifetime. Here bimolecular quenching reactions of  $\text{T}_1$  were assumed to be negligible because of the absence of triplet energy acceptors. The phosphorescence decay was measured at the monitor wavelength of 435 nm with nitrogen laser excitation at 337 nm and the decay curves are depicted in Fig. 2. We observed that  $\tau_{\text{T}} = 2.6\text{ s}$  measured for ECZ in KL at 296 K is 39 times larger than  $\tau_{\text{T}} = 67\text{ ms}$  in KY:<sup>†</sup> in other words, the rate of radiationless deactivation of  $\text{T}_1$  is significantly reduced in the zeolite KL. Thus the large value of  $\tau_{\text{T}}$  must be responsible for the increased  $\Phi_{\text{P}}$  in KL. We assume that the value of  $\Phi_{\text{ST}}$  is not much altered by inclusion in KL compared with that of  $\Phi_{\text{ST}}$  in KY on the basis of a similar fluorescence decay rate of ECZ in both KL and KY (ESI Fig. S1<sup>†</sup>) and a similar relative yield of the triplet state of ECZ in both zeolites, assuming that the value of the molar absorption coefficient for a T–T absorption is unaffected by the zeolite hosts. Therefore, we believe that the channels of zeolite KL provide a rigid environment that suppresses the nonradiative deactivation process of the phosphorescent state, even at ambient temperature, in analogy with solid media at low temperature.

For ECZ, a tight fit into the channel is important since the contribution of phosphorescence is appreciably reduced when NaKL is used instead of KL (See Fig. 1D). In the zeolite L, five positions are found for the extra-framework cations *i.e.* sites A, B, C, D, and E. However, only site D cations are located in the 12R straight channels: precisely, on the walls of the main channels (see Chart 2).<sup>13</sup> Thus the cations in site D are exchangeable at room temperature and it is most likely that the cations at site D were actually exchanged with  $\text{Na}^+$  in the present preparation of the NaKL. In each unit cell of the zeolite L channel there are 6 equivalent D sites and an average of 3.6 of the sites are occupied by the cations.<sup>13</sup> In the present

<sup>†</sup> The phosphorescence lifetime of 9-methylcarbazole, an analogue of ECZ, at 77 K was reported to be 7.0 s (S. L. Murov, I. Carmichael and G. L. Hug, *Handbook of Photochemistry*, Marcel Dekker, New York, 2nd edn., 1993, p. 136) that is comparable with the present result at room temperature.

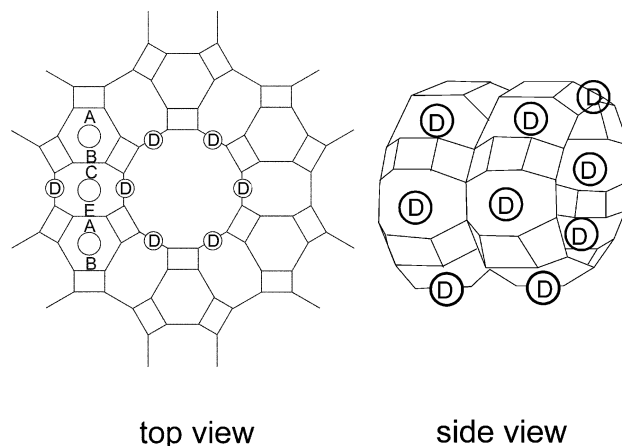


**Chart 2** Pictorial representation of the positions of the cations in zeolite L. Site D cations are located on the walls of main channels and accessible to molecules adsorbed in the channels.

NaKL, 47% of the cations is equivalent to 4.2 per unit cell, well over 3.6. The physical consequence of the cation exchange of  $\text{Na}^+$  for  $\text{K}^+$  is the reduction in cation size, providing more room for guest species in the channels, and a greater charge density leading to an enhanced binding ability to guest organic molecules. The former can be responsible for the decreased phosphorescence intensity of ECZ in NaKL by affording motional freedom to the guest species. The extra pore volume gained by the  $\text{Na}^+$ -exchange of the zeolite KL was 10% as measured by the adsorption of  $\text{H}_2\text{O}$  at 296 K and at a relative humidity of 90%.

We also considered the possibility of the cation–N-atom interaction in the ECZ–zeolite L complex as another origin of the reduced intersystem-crossing rate for ECZ. A molecular orbital calculation with the Spartan program (STO-3G basis set) for the complex of ECZ with  $\text{K}^+$  and  $\text{Na}^+$  showed that the attractive interaction is formed between both the cations and the nonbonding electrons on the N-atom. However, a difficulty arises in the explanation of the observed decreasing phosphorescence intensity on going from  $\text{K}^+$  to  $\text{Na}^+$  (Fig. 1), despite the calculated interaction energy being larger for  $\text{Na}^+$  with higher charge density than for  $\text{K}^+$ . It is also difficult to explain why the intensity of phosphorescence is weak in the zeolites NaY and KY in which the cation–N interaction can be operative. Furthermore, the observation of RTP was made for plain aromatics such as naphthalene (See Fig. 7B1, below) and phenanthrene (ESI Fig. S2<sup>†</sup>) in KL but not in NaKL, showing the minor contribution of the cation–N interaction to the phosphorescence.

Factors affecting the enhanced phosphorescence emission were investigated. The phosphorescence intensity of ECZ in the zeolite KL was markedly reduced in the hydrated zeolite. Aromatic species such as benzene in the main channels have been suggested to be adsorbed in a capping position above the type D cations<sup>14</sup> through the cation– $\pi$  interaction,<sup>15</sup> *i.e.* the interaction between the cation and the  $\pi$ -electron density of the benzene molecule. Water molecules interact strongly with the zeolite surfaces such as framework oxygens and extra framework cations, and interfere with the adsorption of guest species, leading to the liberation of the guest species. Thus ECZ molecules may acquire high mobility in hydrated zeolites,<sup>16</sup> which may lead to reduced phosphorescence intensity. Notably, the phosphorescence intensity change for the hydration–dehydration cycle is completely reversible, suggesting that the observation of phosphorescence is neither an artifact nor due to photochemical reactions. Furthermore, the loading level of the guest species should be kept minimal for the observation of phosphorescence. This minimizes the

occurrence of additional bimolecular deactivation processes such as excimer formation and other quenching processes.

RTP in zeolite KL is much more intense for ECZ than for a few other aromatic species including naphthalene and phenanthrene. We additionally observed an intense RTP for 1,2,4,5-tetracyanobenzene (ESI Fig. S3†). The advantage of ECZ over the other species employed here seems to be the most appropriate matching of its molecular dimension ( $0.96 \times 0.79 \times 0.33$  nm)<sup>§</sup> with the channel size of zeolite KL.

## 2. Formation of intermolecular dimers of biphenyl, naphthalene, and anthracene in zeolite L

Fig. 3 compares the loading-dependent emission spectra (corrected) of biphenyl adsorbed in zeolite KL with those in NaY. In zeolite KL, a fluorescence spectrum similar to that of biphenyl in dilute solution is solely observed at low loadings. Note that biphenyl molecules were assumed to be adsorbed inside the channels, not on the outer surfaces of zeolite KL, based on the maximum loading level that is more than 500 times larger than that observed in NaA. With an increase in the loading level, a broad and featureless emission band with a peak at  $28\,000\text{ cm}^{-1}$  ( $357\text{ nm}$ ) was measured at the expense of the biphenyl fluorescence band that has a peak at  $32\,100\text{ cm}^{-1}$  ( $312\text{ nm}$ ). The new emission band was reasonably ascribed to the excimer emission of biphenyl on the basis of the peak position<sup>17</sup> and the concentration-dependent increase in intensity. Inspection of the excitation spectra (Fig. 4) revealed that a cofacial dimer of biphenyl in the ground state is formed inside the straight channels of zeolite KL. We rationalize that this dimer gives rise to the excimer emission since an appreciable bathochromic shift is observed for the lowest energy band of the excitation spectrum of the excimer band with respect to that of the monomer band, as depicted in Fig. 4. The feasible observation of the excimer emission in zeolite L can qualitatively be understood by the channel shape enforcing a collinear conformation favorable for the formation of the intermolecular dimer. Interestingly, no intermolecular excimer was formed from biphenyl in solution upon photoexcitation; on the other hand, the intramolecular excimer of 1,3-dibiphenylpropane was observed,<sup>17</sup> suggesting the importance of conformational regulation in the excimer formation of biphenyl because of the weak transannular interaction.

In contrast, no excimer was detected for biphenyl in NaY under the present experimental conditions, as also shown in Fig. 3A. For NaY, the pore volume ( $0.378\text{ cm}^3\text{ g}^{-1}$ ) measured with nitrogen adsorption at liquid nitrogen temperature is 2.5 times greater than that of KL ( $0.15\text{ cm}^3\text{ g}^{-1}$ ). However, the larger pore volume is not the only cause of the absence of excimer formation in NaY since no sign of the excimer emission was detected in NaY, even at a loading 10 times as large as in KL. Rather, the large spherical shape that provides conformational flexibility for the guest species within the cages of NaY must be a critical factor that disallows formation of the associated dimer.

The effect of guest molecular size–channel diameter relationship on the associated dimer formation was further investigated by incorporating anthracene ( $0.98 \times 0.56 \times 0.33$  nm) and naphthalene ( $0.73 \times 0.56 \times 0.33$  nm). These molecules have a slightly larger width (short axis length) than biphenyl ( $0.91 \times 0.49 \times 0.33$  nm), but are still slim enough to fit in the straight channels of the zeolite L. We found that naphthalene fits more tightly into the channels than biphenyl because zeolite KL samples doped with sublimed naphthalene at room

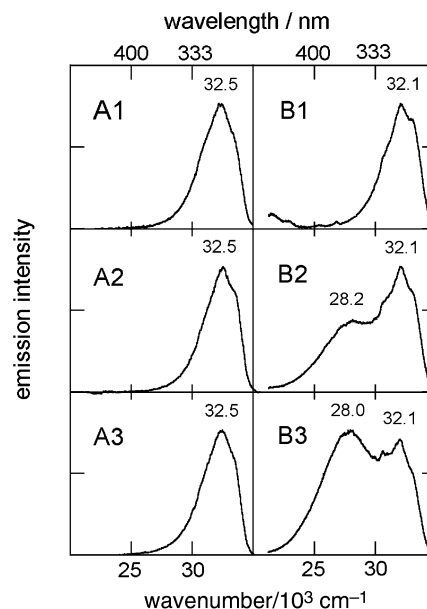


**Fig. 3** Corrected emission spectra of biphenyl adsorbed in zeolites NaY (A) and KL (B) at various loading levels: (A1)  $1.0 \times 10^{-6}$ ; (A2)  $1.0 \times 10^{-5}$ ; (A3)  $1.0 \times 10^{-4}$ ; (B1)  $1.0 \times 10^{-6}$ ; (B2)  $1.6 \times 10^{-5}$  and (B3)  $1.0 \times 10^{-4}$  mol g<sup>-1</sup>. Excitation wavelength was 265 nm ( $37\,700\text{ cm}^{-1}$ ). Cut-off filters were employed both for the excitation and emission beams and the contribution of scattered light was minimized.

temperature gave a broad and structureless emission spectrum that suggests the formation of aggregates on the outer surfaces; however, sublimed and annealed (at  $100\text{ °C}$  for more than 24 h) samples gave an emission spectrum with vibronic structures reminiscent of naphthalene monomer in dilute solution. This means that the molecules have diffused into the channels assisted by thermal energy. Similar adsorption behavior was observed for anthracene. The adsorption of anthracene and naphthalene was carried out from n-hexane solution and their spectroscopic properties were investigated. A close scrutiny of the absorption and emission spectra disclosed a certain difference in the photophysical behavior between anthracene and naphthalene.

The absorption spectrum of anthracene is markedly modified when adsorbed into the zeolite KL as shown in Fig. 5

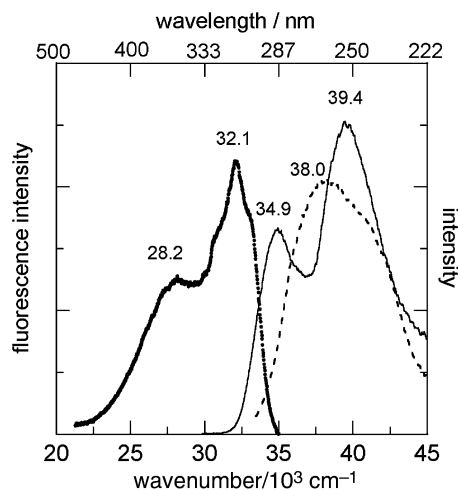


**Fig. 4** Excitation spectra of  $1.6 \times 10^{-5}$  mol g<sup>-1</sup> biphenyl adsorbed in KL. Solid line represents the spectrum for the excimer emission (monitor wavenumber:  $28\,200\text{ cm}^{-1}$ ) and dashed line for the monomer emission (monitor wavenumber:  $32\,100\text{ cm}^{-1}$ ). Dotted line shows the emission spectrum excited at  $40\,000\text{ cm}^{-1}$  ( $250\text{ nm}$ ).

<sup>§</sup> Approximate molecular dimensions (length  $\times$  width  $\times$  thickness) were estimated from the sum of the van der Waals radii of the atoms constituting each molecule. The geometry of the molecules was optimized with a molecular orbital calculation program “Spartan” (Wavefunction) using the STO-3G basis set.

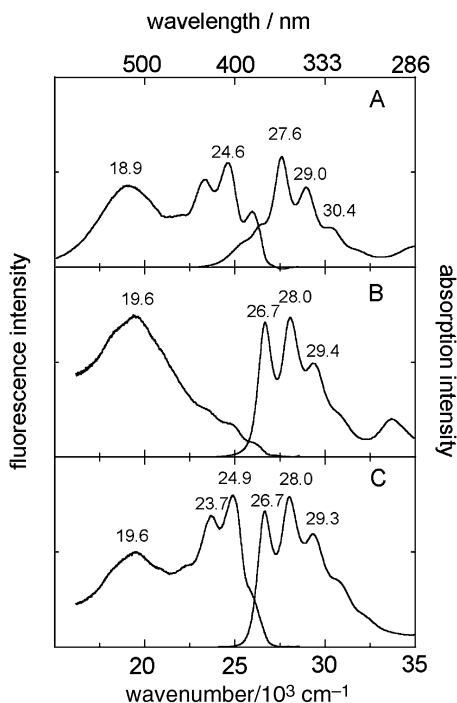


**Fig. 5** Absorption and corrected emission spectra of anthracene in adsorbed systems: (A)  $4.0 \times 10^{-6} \text{ mol g}^{-1}$  adsorbed in zeolite KL; (B)  $> 5.0 \times 10^{-6} \text{ mol g}^{-1}$  adsorbed on the outer surfaces of zeolite NaA; (C)  $1.0 \times 10^{-4} \text{ mol g}^{-1}$  adsorbed in zeolite NaY. Anthracene was adsorbed on NaA by sublimation followed by annealing at  $150^\circ\text{C}$ . Cut-off filters were employed for the measurement of emission spectra and the contribution of scattered light was minimized.

(see Fig 5A for KL system): the absorption band extends deep into the lower energy and the lowest energy vibronic band is notably diminished. This remarkable spectral shape is reminiscent of anthracenophane<sup>18</sup> in which a strong interannular interaction is expected between the two rings due to the short distance between them. Indeed, the excimer emission was observed with a peak position at  $18\,900 \text{ cm}^{-1}$  ( $530 \text{ nm}$ ) together with a monomer emission on photoexcitation even at a low loading level of  $2.0 \times 10^{-6} \text{ mol g}^{-1}$  that is sufficiently smaller than the unit cell concentration of  $4.0 \times 10^{-4} \text{ mol g}^{-1}$  for KL. On the contrary, solution-like absorption spectra were recorded for anthracene in the large pores of NaY and the absorption intensity increased with the loading level. The emission spectra observed in NaY are dependent on the loading level: at loadings less than  $1 \times 10^{-5} \text{ mol g}^{-1}$ , only a monomer-like fluorescence envelope is observed while the contribution of the emission band ascribable to the excimer ( $19\,600 \text{ cm}^{-1}$ ) increased at the expense of the monomer emission with increasing loading level up to  $1 \times 10^{-3} \text{ mol g}^{-1}$  (Fig. 5C). Fig. 5B gives the absorption and fluorescence spectra of anthracene accumulated on the outer surfaces of zeolite NaA by sublimation. Obviously, both the absorption and fluorescence spectra are different from those of anthracene inside the channels of the zeolite KL although they are similar to those of anthracene included in NaY. Note, however, that the fluorescence spectrum on NaA surfaces is entirely of the excimer, even at low loading less than  $5 \times 10^{-6} \text{ mol g}^{-1}$  whereas the loading-dependent spectral change from the monomer to the excimer is clearly observed in NaY. Additionally, the maximum loading level attained by adsorption from solution is more than 1000 times less in NaA than in NaY, indicating saturation of adsorption in NaA at very low loadings. Thus we concluded that anthracene molecules are intercalated in the channels of the zeolite KL as well as in the supercages of NaY, despite the fact that the absorption spectra in KL are severely distorted.

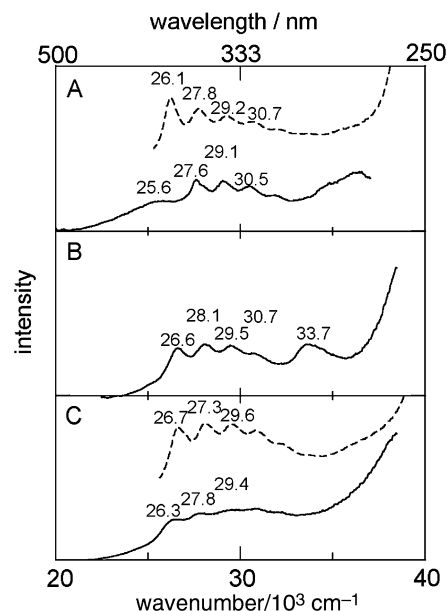


**Fig. 6** Excitation spectra of anthracene adsorbed in KL, on NaA and in NaY:  $4.0 \times 10^{-5} \text{ mol g}^{-1}$  in KL; (B)  $> 5.0 \times 10^{-6} \text{ mol g}^{-1}$  on NaA; (C)  $1.0 \times 10^{-4} \text{ mol g}^{-1}$  in NaY. Solid line represents the spectrum for the excimer emission and dashed line for the monomer emission.

Although the contribution of the excimer emission increased at the expense of the monomer fluorescence with an increase in loading level,<sup>¶</sup> the shape of the absorption spectrum changed only slightly at high loadings (See ESI Fig. S4†). Close inspection of the excitation spectra, however, revealed that associated dimers are actually formed in the ground state. Fig. 6 shows the excitation spectra (uncorrected) of both the monomer and the excimer emission. The excitation spectrum monitored at the excimer peak position ( $18\,900 \text{ cm}^{-1}$ ) in KL is distinguished from that observed at the position of monomer emission ( $24\,600 \text{ cm}^{-1}$ ) by the absence of an unambiguous peak at wavenumbers smaller than  $27\,000 \text{ cm}^{-1}$ , *e.g.*, the peak at  $26\,100 \text{ cm}^{-1}$  ( $383 \text{ nm}$ ) in the excitation spectrum of the monomer emission (Fig. 6A). Moreover, the excitation spectrum monitored at  $18\,900 \text{ cm}^{-1}$  has a spectral shape similar to that of the ground state absorption spectrum of anthracene in KL, indicating that the dimer is actually responsible for the distorted absorption spectrum of anthracene in the zeolite KL. This deduction is further supported by the observation of recovery of the normal absorption spectrum of anthracene monomer accompanied by the disappearance of the excimer emission on hydration of the zeolite KL (See ESI Fig. S5†). We showed previously that the hydration of zeolite causes weakening of the interaction between the zeolite and the guest species, leading to the dissociation of the dimer due to its repulsive nature.<sup>8b</sup> Note that the spectral change due to the hydration–dehydration cycle is completely reversible.

The peak position of  $18\,900 \text{ cm}^{-1}$  ( $530 \text{ nm}$ ) for the excimer emission in KL with a fluorescence lifetime of  $50 \text{ ns}$  at  $296 \text{ K}$  (ESI Fig. S6†) suggests that the two anthracene molecules adopt a cofacial arrangement with their centers offset: one anthracene is offset relative to the other by one benzene ring along the long axis so that two phenyl rings overlap. Previously, various types of anthracene dimer model compounds

<sup>¶</sup> The emission spectra of anthracene monomer adsorbed in the zeolite suffered self-absorption. This is caused by the high concentration in the channels, not by the formation of aggregates on the outer surfaces. For instance, the lowest loading of  $2.0 \times 10^{-6} \text{ mol g}^{-1}$  corresponds to  $0.013 \text{ mol dm}^{-3}$  and a typically high loading of  $1.0 \times 10^{-4} \text{ mol g}^{-1}$  to  $0.67 \text{ mol dm}^{-3}$  in the zeolite KL, considering a pore volume of  $0.15 \text{ cm}^3 \text{ g}^{-1}$ .

were synthesized and their spectroscopic properties such as the emission spectra and lifetimes dependent on the various conformation of two anthracene moieties were extensively investigated.<sup>19</sup> On the basis of those studies we presume that the dimer structure of anthracene in the zeolite KL is analogous to that achieved for [2.2](1,4)(9,10)anthracenophane or 1-(1-anthryl)-3-(9-anthryl)propane.

The excimer emission of anthracene was only observed in NaY at sufficiently high loadings,  $> 1 \times 10^{-4} \text{ mol g}^{-1}$  whereas in the zeolite KL, excimer emission was observed at a very low loading such as  $2.0 \times 10^{-6} \text{ mol g}^{-1}$ . In NaY, several different spectroscopic properties from those in the KL system are noted. No appreciable difference was observed in the absorption spectra from those of the solution. The excitation spectra of the excimer emission (See Fig. 6C) are slightly red-shifted but the spectral envelopes are similar to those of monomer emission, a remarkably different observation from that in the KL zeolite. In addition, as we have reported previously,<sup>8</sup> the peak position of the excimer emission,  $19\,600 \text{ cm}^{-1}$  (510 nm) at room temperature shifted to  $21\,000 \text{ cm}^{-1}$  (475 nm) at 77 K. This observation implies that geometrical relaxation in the excited state is feasible in the large spherical cages of NaY. Notably, no spectral shift was observed for the excimer emission of anthracene in KL at 77 K, presumably because of the tight fit. Overall, the significantly altered absorption spectra characteristic of anthracene in the zeolite KL can be ascribed to a stronger interannular interaction forced by confinement in the narrow channels of zeolite L compared with that in the large pores of NaY.

We also observed excimer emission bands arising from intermolecular dimers of naphthalene intercalated into the zeolite KL. However, the emission cannot be assigned to a typical sandwich-type excimer that has a peak at *ca.*  $25\,000 \text{ cm}^{-1}$  (400 nm) in solution<sup>20</sup> but is assignable to the second excimer with a peak at  $27\,800\text{--}27\,000 \text{ cm}^{-1}$  (360–370 nm) in which only one benzene ring of the two naphthalene molecules overlaps.<sup>21</sup> Fig. 7 compares the loading dependent emission spectra of naphthalene adsorbed in KL with those of naphthalene in NaY. In the zeolite NaY, the loading dependent behavior is reminiscent of that in solution: a purely monomer-like fluorescence spectrum was recorded at low loadings and

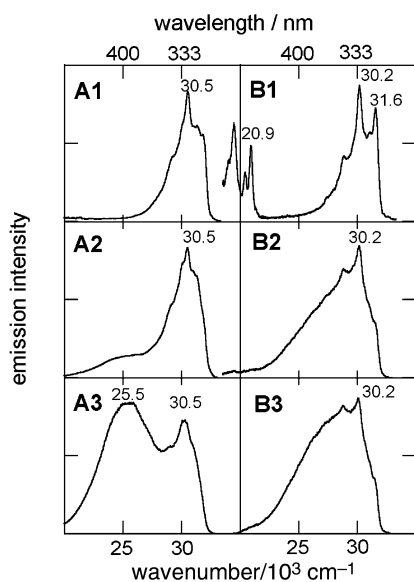


**Fig. 7** Corrected emission spectra of naphthalene adsorbed in zeolites NaY (A) and KL (B) at various loading levels: (A1)  $1.0 \times 10^{-5}$ ; (A2)  $1.0 \times 10^{-4}$ ; (A3)  $5.0 \times 10^{-4}$ ; (B1)  $2.0 \times 10^{-6}$ ; (B2)  $6.0 \times 10^{-5}$  and (B3)  $1.2 \times 10^{-4} \text{ mol g}^{-1}$ . Excitation wavelength was  $37\,000 \text{ cm}^{-1}$  (270 nm). Cut-off filters were employed both for excitation and emission beams and the contribution of scattered light was minimized.

the contribution of the excimer emission with a peak at  $25\,500 \text{ cm}^{-1}$  (392 nm) increased at the expense of the monomer emission as the loading increases (Fig. 7A).<sup>9</sup> The loading-dependent spectral change is also observed in zeolite KL, however, the peak position of the excimer emission in KL is so close to that of the monomer emission that the spectra cannot be well-separated, even at a high loading of  $1.2 \times 10^{-4} \text{ mol g}^{-1}$  (Fig. 7B). A more decisive experiment that can prove the presence of the excimer band buried in the monomer emission band is the measurement of the fluorescence decays at different wavelengths. As shown in Fig. 8, the emission decay observed at  $30\,200 \text{ cm}^{-1}$  (331 nm) differs appreciably from that at  $25\,000 \text{ cm}^{-1}$  (400 nm) at a naphthalene loading of  $6.0 \times 10^{-5} \text{ mol g}^{-1}$ . Thus we conclude that zeolite KL enforces geometrical constraints to form the unstable second excimer of naphthalene while zeolite Y allows enough room for naphthalene pairs to form the stable sandwich excimer.

The partially overlapped structure with collinear and offset geometry of the naphthalene dimer characteristic in zeolite KL deserves comment. Previously investigated intermolecular and intramolecular excimers of naphthalene are mostly of the sandwich-type structure. One exception is the excimer in which two naphthalene rings are twisted with each other in such a fashion that only one benzene ring overlaps,<sup>21</sup> observed for a solution of 1,3-bis(4-methoxy-1-naphthyl)propane and 1,3-bis(4-hydroxy-1-naphthyl)propane. Such a configuration cannot be adopted by the intermolecular naphthalene dimer in the narrow straight channels of the zeolite KL; instead, collinear conformation will be forced. This conformation is similar to that of a model compound, anti-[2,2] paracyclonaphthane prepared and characterized spectroscopically by Froines and Hagerman.<sup>22</sup>

We observed that the narrow channels of zeolite KL force biphenyl, naphthalene, and anthracene to associate to form dimers with collinear conformation and, especially for anthracene, the two rings are remarkably close due to the confinement effect. We also observed that the exchange of  $\text{K}^+$  ions with  $\text{Na}^+$  in the main channel of the zeolite L drastically affects the association of these guest species. For anthracene, another type of intermolecular excimer structure ascribable to a partially-overlapped geometry involving one benzene ring of the two anthracene molecules is observed with a peak at  $21\,200 \text{ cm}^{-1}$  (472 nm) at high loadings in NaKL (Fig. 9). This conformation is known to occur in a model compound, anti-[2.2](1,4)anthracenophane.<sup>19</sup> On the contrary, the excimer emission of naphthalene is totally absent, irrespective of the loading level: even at a loading as high as  $2.3 \times 10^{-4} \text{ mol g}^{-1}$

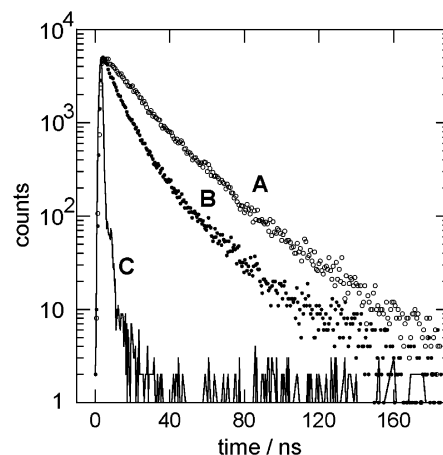


**Fig. 8** Fluorescence decay curves of  $6.0 \times 10^{-5} \text{ mol g}^{-1}$  naphthalene adsorbed in KL excited at 270 nm ( $37\,000 \text{ cm}^{-1}$ ) and observed at two different wavelengths: (A) 400 nm ( $25\,000 \text{ cm}^{-1}$ ); (B) 331 nm ( $30\,200 \text{ cm}^{-1}$ ); (C) excitation lamp profile.

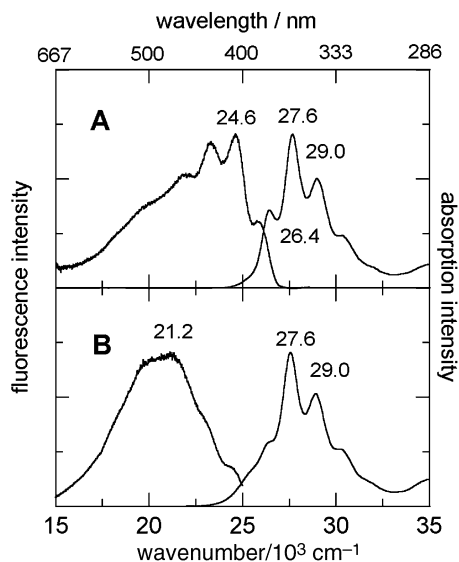


**Fig. 9** Absorption and corrected emission spectra of anthracene adsorbed in zeolite NaKL at two loading levels: (A)  $2.0 \times 10^{-6}$  mol  $\text{g}^{-1}$ ; (B)  $6.0 \times 10^{-5}$  mol  $\text{g}^{-1}$ . Excitation wavelength: 340 nm ( $29\,400$   $\text{cm}^{-1}$ ). Cut-off filters were employed for the measurement of emission spectra and the contribution of scattered light was minimized.

(Fig. 10). Thus the conformation of the dimers of anthracene and the association of naphthalene in the channels of zeolite L are both largely dependent on the charge-compensating cations. It is interesting to note that the emission spectrum assignable to the second excimer (partially overlapped structure) is detected in NaKL (ESI Fig. S7†) for highly loaded biphenyl that gave excimer emission ascribable to a fully overlapped geometry in KL (Fig. 3B). This finding shows that biphenyl behaves more like anthracene than naphthalene for the cation exchange. Thus, the molecular dimension of the guest species is another important factor for the observed association and photophysical behavior dependent on the

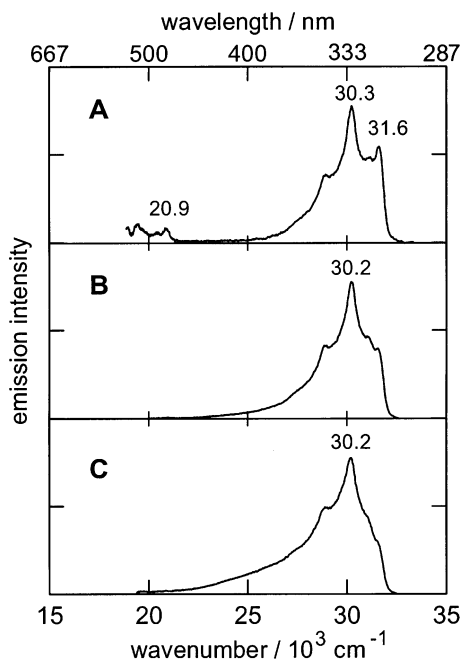


**Fig. 10** Corrected emission spectra of naphthalene adsorbed in zeolite NaKL at various loading levels: (A)  $2.0 \times 10^{-6}$ ; (B)  $1.0 \times 10^{-4}$  and (C)  $2.3 \times 10^{-4}$  mol  $\text{g}^{-1}$ . Excitation wavelength: 270 nm ( $37\,000$   $\text{cm}^{-1}$ ). Cut-off filters were employed both for the excitation and emission beams and the contribution of scattered light was minimized.

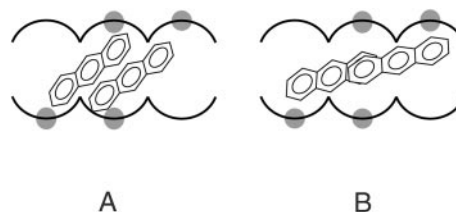


**Chart 3** Geometry of associated anthracene molecules in the channel depending on the cation: (A) KL; (B) NaKL.

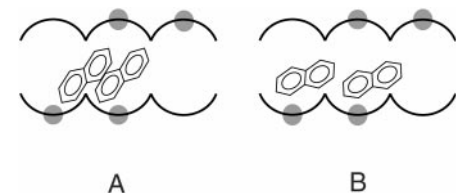


**Chart 4** Geometry of naphthalene molecules in the channel depending on the cation: (A) KL; (B) NaKL.

cations. Nevertheless, the present findings open a new aspect that the distribution and conformation of guest molecules within the channels can be controlled in terms of the charge compensating cations. Such a control by modifying the cations is not possible in the large spherical-pore zeolite Y.

Here we discuss the present observation of the excimers with various overlapping structures confined within the zeolite L depending on the charge compensating cations. We propose that the conformation of associated anthracene molecules both in zeolite KL and in NaKL can be depicted in Chart 3. A similar situation to that of anthracene is expected for biphenyl. Also the adsorption feature of naphthalene is dependent on the cation, as shown in Chart 4. The basic assumption is that two molecules cannot occupy the same unit cell in which the geometry is such that the long molecular axis is required to be perpendicular to the  $c$ -axis since the driving force of the adsorption of aromatic species in the channels is the cation- $\pi$  interaction with the charge balancing cations as mentioned above. For the proper interaction to operate, the molecular plane of the guest aromatic molecules should be placed in a face to face geometry with the cations. This conformation can easily be attained by benzene but not feasibly by its larger analogues, anthracene and naphthalene, due to the geometrical restrictions imposed by the channel walls. Thus these molecules are forced to lie tilted against the  $c$ -axis which is along the main channel direction. We assume that the molecular planes of these species are severely tilted in KL compared with those in NaKL in which the larger cation- $\pi$  interaction due to the larger charge density of  $\text{Na}^+$  than  $\text{K}^+$  may attract the adsorbed species at a closer distance, enforcing a parallel geometry to the  $c$ -axis of the main channels. The spectroscopic evidence does not give direct proof of this assumption, however, the adsorption isotherm study, in which the maximum adsorbed amount is observed to be much larger in NaKL than in KL, gives indirect proof. It is reasonable to assume that a greatly tilted geometry can easily cause congestion and end up with a smaller amount of adsorption. A more precise picture could be obtained from a crystallographic study<sup>2a</sup> or fluorescence microscopy of a single crystal zeolite with a polarized light.<sup>6c</sup> Such studies will be conducted in the near future.

|| The effect of a 10% increase in pore volume by the cation exchange with  $\text{Na}^+$  for  $\text{K}^+$  is minor and contributes less to the present observation of the conformational change of the guest molecules dependent on the cations.

### 3. Comparison of neutral aromatics with cationic dyes in zeolite L

Cationic dyes have been the most intensively investigated species in the zeolite L system; thus it is pertinent to make a comparison with the present results for neutral species. Calzaferri and coworkers<sup>3a</sup> have shown that Thionine (TH<sup>+</sup>) that has a slightly larger short axis length than anthracene can be incorporated into the channels of KL in purely monomeric form. In contrast, Methylene Blue (MB<sup>+</sup>) in which the two amino groups of TH<sup>+</sup> are exchanged with dimethylamino groups cannot go into the channels, possibly due to size discrimination by the channel aperture, but forms dimers and aggregates on the outer surfaces. It is noteworthy that anthracene forms dimers within the channels despite the meagre difference in molecular size from TH<sup>+</sup>. Thus the channels of zeolite L are very sensitive to the molecular size of guest species in controlling inclusion and association phenomena, regardless of the charge on the guest species. Such sensitivity cannot be anticipated for zeolite Y.

MV<sup>+</sup> cation radicals can readily dimerize to form [MV<sup>+</sup>]<sub>2</sub> at high concentrations in dehydrated KL but not in dehydrated NaY in which the collinear conformation is not enforced because of the available space in the supercages.<sup>5</sup> This behavior is quite reminiscent of that of biphenyl which has a similar molecular size. Thus it seems that molecular association in the zeolite channels and cavities depends solely on the size of the guest species, irrespective of the charge. However, an important difference is the association in hydrated zeolites. While an enhanced association was observed for the cationic dyes including MV<sup>+</sup>,<sup>5</sup> and MB<sup>+</sup>,<sup>3b</sup> diminished association was observed for the neutral species in both zeolite L and Y. Hydrophobic interaction is ascribed to a major driving force for the aggregation of dyes in aqueous media. On the other hand, the polarization of molecules caused by the interaction with the cations can be responsible for the association of the neutral species within the zeolites.<sup>8,23</sup>

Cationic dyes, Pyronine (Pyr<sup>+</sup>) and Oxonine (Oxo<sup>+</sup>) as well as TH<sup>+</sup> can be incorporated into zeolite KL in a monomeric form with a homogeneous distribution at high loading levels.<sup>6</sup> In contrast, the tendency of association of neutral aromatic species prevailed in the zeolite KL. However, the association of naphthalene was prevented in Na<sup>+</sup>-exchanged zeolite L and much higher loading was attained, suggesting the occurrence of homogeneous distribution throughout the channels. This was obviously attained by the compartmentalization effect exerted by the cations that interplay with the guest species.

Accordingly, neutral aromatics and cationic dyes alike tend to go into the channels and form aggregates if geometrically allowed. Nevertheless, one of the different features of the neutral species is the dissociation on hydration, the tendency to give rise to heterogeneous distribution in the dehydrated zeolite and the redistribution on the cation exchange.

### Summary

We investigated, mainly with emission spectroscopy the photophysical properties of neutral aromatic molecules incorporated inside the straight channels of zeolite L. The photophysics in the channel system was remarkably altered compared with that observed in large spherical-pore faujasite zeolites or in solution, which suggests better ways of controlling the excited-state properties utilizing the zeolite L. The fluorescence spectroscopy was sensitive enough to detect the details of the association behavior of aromatic molecules such as biphenyl, anthracene, and naphthalene. Of these, perhaps the most remarkable observation is the formation of anthracene dimer that has appreciably short interannular separation, comparable to that of anthracenophane, as a consequence of the tight

fit of two anthracene molecules into the narrow channels. Additionally, we found that the conformation of associated dimers of anthracene and the association behavior of naphthalene are governed by the charge compensating cations in the channels, which open ways of manipulating the distribution and conformation of adsorbed species. We also found that the tight fit of molecules in the narrow channels leads to the remarkably intense room temperature phosphorescence that is hardly ever observed in other media. The example of the concept of tight-fit was best realized for the 9-ethylcarbazole-KL pair. The finding of RTP in the channels is also regarded as an example of the control of photophysics in terms of the cations that can fine-tune the size of both the channel aperture and the cylinder. Accordingly, we shed light on a critical role of the charge-compensating cations in the adsorption interaction and photophysical properties of neutral guest species intercalated in the channel-type zeolite L.

### Acknowledgement

Financial support by Iketani Science and Technology Foundation (grant No.011023-A) is gratefully acknowledged. The technical assistance of Mr. Kazuyuki Takehira of Gunma University is gratefully acknowledged. We thank Professor Thomas Ebbesen of Universite Louis Pasteur (Strasbourg) for stimulating discussion. Our thanks are also due to the Royal Society of Chemistry for providing S. H. with a grant (Journals Grants for International Authors # 00 06/250) which made possible the travel to Strasbourg.

### References

- (a) J. K. Thomas, *Chem. Rev.*, 1993, **93**, 301; (b) K. B. Yoon, *Chem. Rev.*, 1993, **93**, 321; (c) V. Ramamurthy, P. L. akshiminasimham, C. P. Grey and L. J. Johnston, *Chem. Commun.*, 1998, 2411; (d) J. C. Sciano and H. Garcia, *Acc. Chem. Res.*, 1999, **32**, 783; (e) G. Calzaferri, D. Brühwiler, S. Megelski, M. Pfenniger, M. Pauchard, B. Hennessy, H. Maas, A. Devaux and U. Graf, *Solid State Sci.*, 2000, **2**, 421; (f) N. J. Turro, *Acc. Chem. Res.*, 2000, **33**, 637; (g) K. B. Yoon, in *Solid State and Surface Photochemistry*, ed. V. Ramamurthy and K. S. Schanze, Marcel Dekker, New York, 2000, ch. 4, p. 143; (h) S. Hashimoto, in *Solid State and Surface Photochemistry*, ed. V. Ramamurthy and K. S. Schanze, Marcel Dekker, New York, 2000, ch. 5, p. 253.
- (a) B. Hennessy, S. Megelski, C. Marcolli, V. Shklover, C. Bärlocher and G. Calzaferri, *J. Phys. Chem. B*, 1999, **103**, 3340; (b) Y. S. Park, Y. S. Um and K. B. Yoon, *J. Am. Chem. Soc.*, 1999, **121**, 3193.
- (a) G. Calzaferri and N. Gfeller, *J. Phys. Chem.*, 1992, **96**, 3428; (b) V. Ramamurthy, D. R. Sanderson and D. F. Eaton, *J. Am. Chem. Soc.*, 1993, **115**, 10438.
- (a) H. J. D. Mcmanus, C. Finel and L. Keavan, *Radiat. Phys. Chem.*, 1995, **45**, 761; (b) M. Alvaro, H. Garcia, S. Garcia, F. Márquez and J. C. Sciano, *J. Phys. Chem. B*, 1997, **101**, 3043.
- Y. S. Park, K. Lee, C. Lee and K. B. Yoon, *Langmuir*, 2000, **16**, 4470.
- (a) F. Binder, G. Calzaferri and N. Gfeller, *Proc. Indian Acad. Sci.*, 1995, **107**, 753; (b) N. Gfeller and G. Calzaferri, *J. Phys. Chem. B*, 1997, **101**, 1396; (c) N. Gfeller, S. Megelski and G. Calzaferri, *J. Phys. Chem. B*, 1998, **102**, 2433; (d) N. Gfeller, S. Megelski and G. Calzaferri, *J. Phys. Chem. B*, 1999, **103**, 1250; (e) S. Megelski, A. Lieb., M. Pauchard, A. Drechsler, S. Glaus, C. Debus, A. J. Meixner and G. Calzaferri, *J. Phys. Chem. B*, 2001, **105**, 25.
- (a) X. Liu and J. K. Thomas, *Chem. Mater.*, 1994, **6**, 2303; (b) M. Pauchard, A. Devaux and G. Calzaferri, *Chem. Eur. J.*, 2000, **6**, 3456.
- (a) S. Hashimoto, N. Fukazawa, H. Fukumura and H. Masuhara, *Chem. Phys. Lett.*, 1994, **219**, 445; (b) S. Hashimoto, S. Ikuta, T. Asahi and H. Masuhara, *Langmuir*, 1998, **14**, 4284.
- (a) S. Hashimoto, T. Mutoh, H. Fukumura and H. Masuhara, *J. Chem. Soc., Faraday Trans.*, 1996, **92**, 3653; (b) S. Hashimoto, *Chem. Phys. Lett.*, 1996, **262**, 292.

- 10 E. Lippert, W. Naegel, I. Siebold-Blankenstein, U. Staiger and W. Voss, *Z. Anal. Chem.*, 1959, **170**, 1.
- 11 (a) J. V. Casper, V. Ramamurthy and D. R. Corbin, *Coord. Chem. Rev.*, 1990, **97**, 225; (b) V. Ramamurthy, J. V. Casper, D. F. Eaton, E. W. Kuo and D. R. Corbin, *J. Am. Chem. Soc.*, 1992, **114**, 3882; (c) V. Ramamurthy, D. F. Eaton and J. V. Casper, *Acc. Chem. Res.*, 1992, **25**, 299; (d) S. Uppili, K. J. Thomas, E. M. Crompton and V. Ramamurthy, *Langmuir*, 2000, **16**, 265; (e) S. Uppili, V. Marti, A. Nikolaus, S. Jockusch, W. Adam, P. S. Engel, N. J. Turro and V. Ramamurthy, *J. Am. Chem. Soc.*, 2000, **122**, 11 025.
- 12 N. J. Turro, *Modern Molecular Photochemistry*, University Science, Mill Valley, CA, 1991, p. 128.
- 13 D. W. Breck, *Zeolite Molecular Sieves*, Krieger, Malabar, 1984, p. 114.
- 14 (a) B. G. Silbernagel, A. R. Garcia, J. M. Newsman and R. Hulme, *J. Phys. Chem.*, 1989, **93**, 6506; (b) J. M. Newsman, *J. Phys. Chem.*, 1989, **93**, 7689.
- 15 (a) R. A. Kumpf and D. A. Dougherty, *Science*, 1993, **261**, 1708; (b) J. C. Ma and D. A. Dougherty, *Chem. Rev.*, 1997, **97**, 1303; (c) J. B. Nicholas, B. P. Hay and D. A. Dixon, *J. Phys. Chem. A*, 1999, **103**, 1394; (d) S. Tsuzuki, M. Yoshida, T. Uchimura and M. Mikami, *J. Phys. Chem. A*, 2001, **105**, 769.
- 16 S. Hashimoto, T. Miyashita and M. Hagiri, *J. Phys. Chem. B*, 1999, **103**, 9149.
- 17 K. A. Zachariasse, W. Kühnle and A. Weller, *Chem. Phys. Lett.*, 1978, **59**, 375.
- 18 J. Ferguson, *Chem. Rev.*, 1986, **86**, 957.
- 19 (a) T. Hayashi, N. Mataga, Y. Sakata, S. Misumi, M. Morita and J. Tanaka, *J. Am. Chem. Soc.*, 1976, **98**, 5910; (b) M. Itoh, K. Fuke and S. Kobayashi, *J. Chem. Phys.*, 1980, **72**, 1417.
- 20 (a) C. A. Parker, *Spectrochim. Acta*, 1963, **19**, 989; (b) B. K. Selinger, *Aust. J. Chem.*, 1966, **19**, 825.
- 21 H. Itagaki, N. Obukata, A. Okamoto, K. Horie and I. Mita, *J. Am. Chem. Soc.*, 1982, **104**, 4469.
- 22 J. R. Froines and P. J. Hagerman, *Chem. Phys. Lett.*, 1969, **4**, 135.
- 23 (a) V. Ramamurthy, D. R. Sanderson and D. F. Eaton, *J. Phys. Chem.*, 1993, **97**, 13 380; (b) K. J. Thomas, R. B. Sunoj, J. Chandrasekhar and V. Ramamurthy, *Langmuir*, 2000, **16**, 4912; (c) S. Hashimoto and S. Ikuta, *J. Mol. Struct. (THEO-CHEM)*, 1999, **468**, 85.